J. RADIAT. RES., 31, 189–206 (1990)

Biological and Physical Dosimeters for Monitoring Solar UV-B Light

YOSHIYA FURUSAWA, KENSHI SUZUKI AND MASAKO SASAKI*

Department of Molecular Biology,
School of Medicine Tokai University, Isehara, Kanagawa 259-11, and
*Institute of Research and Development,
Tokai University, Hiratsuka, Kanagawa 259-12, Japan

(Received October 17, 1989)
(Revised version, accepted April 4, 1990)

Dosimeter/Biological effects/Solar UV-B/Bacteriophage T1/Ozone depletion

A biological dosimetry system for measuring solar UV-B light was established using bacteriophage T1 with *E. coli* Bs-1 as the host cell. Also a new physical UV-B dosimeter was developed which can specifically detect the UV spectral region related to inactivation of phage T1.

Phage T1 is very stable in liquid suspension and it has adequate sensitivity to measure the intensity of solar UV-B. In addition, the survival of phage T1 responded linearly to UV fluences when plotted semi-logarithmic ally. Thus T1 seemed to have characteristic features making it suitable material as a biological dosimeter for sunlight. Outdoor experiments throughout one year showed that the mean amount of solar UV light in summer was about 6 fold larger than that in winter at Isehara (139.5°E, 35.5°N), Japan.

A novel physical dosimeter which responds faithfully to UV-B light under atmospheric conditions on the ground was developed as well. The spectral response was very close to that of biological materials. Readings of this UV-B dosimeter could be converted into the efficiency of sunlight upon biological materials. This instrument is compact; it can also be used as an erythemal dosimeter.

INTRODUCTION

Two important findings were reported recently about the crisis of the ozone layer which surrounds the outermost region of the globe. One is concerned with the ozone hole at the South Pole reported by Chubachi[1] and Farman *et al.*[2] and the other with the total ozone depletion on a whole terrestrial scale according to Solomon *et al.*[3] The ozone layer absorbs UV-B and -C radiation from the sun and protects living organisms on the earth from severe UV damage. In order to protect the ozone layer, the Montreal Protocol[4] which is based on scientific criteria[5] has been accepted at the United Nations Environment Program International Convention. The World Health Organization has also recommended[6] further studies on solar UV radiation to

古沢佳也，鈴木孳之：東海大学医学部，神奈川県伊勢原市望星台　〒259—11
佐々木政子：東海大学開発技術研究所，神奈川県平塚市北金目　〒259—12

improve evaluation of health risks and to establish appropriate protective measures and guidelines. Because of the increasing risk of skin cancer due to increasing exposure to sunlight, a reasonable standard for biological effects by solar UV radiation should be established. So far, harmful effects of UV radiation on the human skin have mostly been evaluated on the basis of erythemal action. Recently a reference action spectrum of erythema[7] and spectral biological effectiveness for exposure limits[8] of UV radiation were reported by the International Commission on Illumination and the World Health Organization, respectively.

Seasonal variation of inactivation efficiency of sunlight was measured with *Bacillus subtilis* spores by Munakata[9] and Tyrrell[10] at Tokyo, Japan and Rio de Janeiro, Brazil, respectively. Also, minimum erythema time of patients with xeroderma pigmentosum was estimated[11] based on readings of 305/365 UV Radiometer (Eisai, Tokyo) and the data of solar spectral irradiance. In order to reasonably evaluate the biological effects of sunlight, it is necessary to measure the intensity of the UV-B region taking its spectral characteristics into account. However, existing physical dosimetry systems ordinarily respond sensitively to wavelengths longer than biologically effective wavelengths. The longer light wavelengths are a major component of natural sunlight but their effect on biological materials is very small. Hence, this sensitivity to longer wavelengths may mask the real biological effects of sunlight which are affected by small changes in the ozone layer. Therefore, a physical dosimeter which has a response spectrum similar to the biological action spectrum is needed. A newly developed dosimeter which is reported here was developed to meet this demand, especially within the solar UV-B region. It is very compact and can be easily carried anywhere.

In parallel with the development of the dosimeter, we examined the capability of bacteriophage T1 as a biological dosimeter for solar UV light by annual measurement of survival at a definite location, in Isehara, Japan. Bacteriophage T1 had several advantages for outdoor use as a biological dosimeter: (1) It was stable for rather a long time in liquid suspension or in dry state. (2) Measurable fractions were killed by exposure to natural sunlight in a daytime. (3) Survival responded linearly to the amount of exposure when they were plotted on a semi-logarithmic scale. (4) Survival could be determined in a short time and without any difficulty. In addition, the cost of survival measurements is very low.

The data showed seasonal changes of the amount of T1-killing sunlight which was assumed to be related to the thickness of the ozone layer through which the light passed.

MATERIALS AND METHODS

Preparation of bacteriophage T1

Escherichia coli B cells were grown overnight in Nutrient Broth (NB) medium (8 g Difco Nutrient Broth, 5 g NaCl and 1 ml 1N-NaOH per litre of distilled water). Eight milliliters of the culture were transferred to 500 ml of 3×D medium (4.5 g KH_2PO_4, 26.5 g Na_2HPO_4-$12H_2O$, 3 g NH_4Cl, 15 g Difco Casamino Acid and 13 g glycerol per litre of distilled water; after autoclave 1.2 ml 1M-$MgSO_4$, 0.15 ml 1M-$CaCl_2$ and 3 ml 1%-gelatin were added) and incubated

at 37°C with aeration. When the cell concentration reached 5×10^8 cells/ml ($O.D._{650} = 0.50$), 2.5×10^{10} p.f.u. (plaque forming unit) of bacteriophage T1 were added into the culture. A small amount of Antifoam-A (Sigma) was added to suppress foaming. Incubation was continued for 3 hours until lysis was complete. Then one ml of chloroform and 2 μg/ml each of DNase and RNase were added, the lysate was incubated for 30 min at room temperature and centrifuged at 4,000 × g for 40 min at 4°C to remove cell debris. The supernatant was ultracentrifuged (70,000 × g for 3 hr at 4°C with 94 ml angle rotor) and the phage pellet was saved. The pellet was resuspended in about 1 ml of T1 buffer (0.3 g KH_2PO_4, 1.5 g Na_2HPO_4-$12H_2O$ per litre of water with $MgSO_4$, $CaCl_2$ and gelatin at final concentrations of 40 μM, 50 μM and 0.0025%, respectively). The phage thus obtained was purified by CsCl step-gradient (densities(ρ) = 1.45, 1.50 and 1.70 in a cellulose nitrate tube) centrifugation (60,000 × g for 2 hr at 4°C with 5 ml swing rotor). The layer between densities of 1.50 and 1.45 was collected by puncturing the side of the tube and then dialyzed against T1 buffer.

Light source and its performances

The Okazaki Large Spectrograph (OLS)[12,13] at the National Institute for Basic Biology, Okazaki, Japan and a CRM-FM Spectro-irradiator[14] (JASCO, Hachioji, Japan) were used as light sources of monochromatic UV; 30 kW Xe short arc lamp equipped with 90 cm × 90 cm grating (1200 grooves/mm, doubly blazed at 250 nm and 500 nm) in OLS and 5 kW Xe short arc lamp operated at 3 kW with 84 mm × 84 mm grating (1200 grooves/mm, blazed at 200 nm) in CRM-FM. Exposure rate in CRM-FM was measured by a TC-CTS thermocouple radio meter (JASCO), which had been calibrated against NBS (National Bureau of Standards, U.S.A.) standard radiometer by JASCO. A silicon photodiode radiometer which had also been calibrated with NBS standard by Hamamatsu Photonics Co. (Hamamatsu, Japan) was used for measurements of exposure rate in OLS. In order to avoid contamination of short wavelength light, we employed UV filters (Hoya, Akishima and/or Toshiba, Tokyo, Japan) when experiments were done at above 290 nm. Purity of the light of OLS with the UV filter as expressed by half-maxima-half-width measured by a P-250 Monochrometer (Nikon, Tokyo) was 2.0 nm, and the intensity of contaminating light with a wavelength 10 nm shorter than the main wavelength was less than 1×10^{-3} of the main light. The fluence rate in OLS at 300 nm was determined to be about 15 W/m^2 with 50 mm entrance slit, 10 mm exit slit and UV-30 (Hoya) filter, and the same rate in CRM-FM was 0.35 W/m^2 with 1 mm entrance slit and 1 mm exit slit.

Measurements of solar irradiance

Solar irradiance wavelengths longer than 400 nm was measured by a MS-801 actinometer (EKO Instruments Trading, Tokyo) which has a flat response from 400 nm to 3000 nm, and solar UV-irradiance (300–400 nm) was measured by a MS-140 UV-radiometer (EKO) which has its peak response at 340 nm. Both meters have a hemispherical cosine angular response. Solar irradiance (300–3000 nm) was calculated by the sum of readings of these two meters. UV-B intensity of the sun expressed in sunburn units (SU) was measured with a R-B meter (Model 5A, Solar Light Co., Philadelphia). One sunburn unit is defined as an equivalent to the minimal erythema dose on Caucasian skin to show a barely perceptible reddening 4–8 hours after

irradiation. Characteristics of the R-B meter were reported in detail by Berger[15].

Irradiation of bacteriophage T1

Stock suspension of phage T1 was diluted to about 10^7 p.f.u./ml with T1 buffer. When it was exposed in OLS, 200 μl of suspension was put into a small plastic cup (7 mm^{ϕ}, 10 mm^{h}). When it was exposed in CRM-FM, 3 ml of suspension was placed into a quartz cell having a light path of 10 mm. Outdoor exposure to natural sunlight was performed in a four-wall quartz cell (10 mm). During exposure, one surface of the cell wall was faced against the sun and followed the sun's projection. Exposure time and readings of R-B meter were recorded and used for the calculation of survival fractions. In every case, sample suspension was cooled by ice-water during irradiation. Portions of the phage suspension were withdrawn at intervals and kept in the dark at 0°C until phage survival measurements were performed. Phage survivals were determined by the agar layer method (final concentration of 1.5% and 0.75% agar was added into the NB medium for agar plates and soft agar, respectively). A repair deficient strain, *E. coli* Bs-1, was used as indicator cells.

DESIGN OF PHYSICAL DOSIMETER

Outline of the newly designed UV-B dosimeter

The main optical system consists of the components shown in Figure 1 and Figure 2:

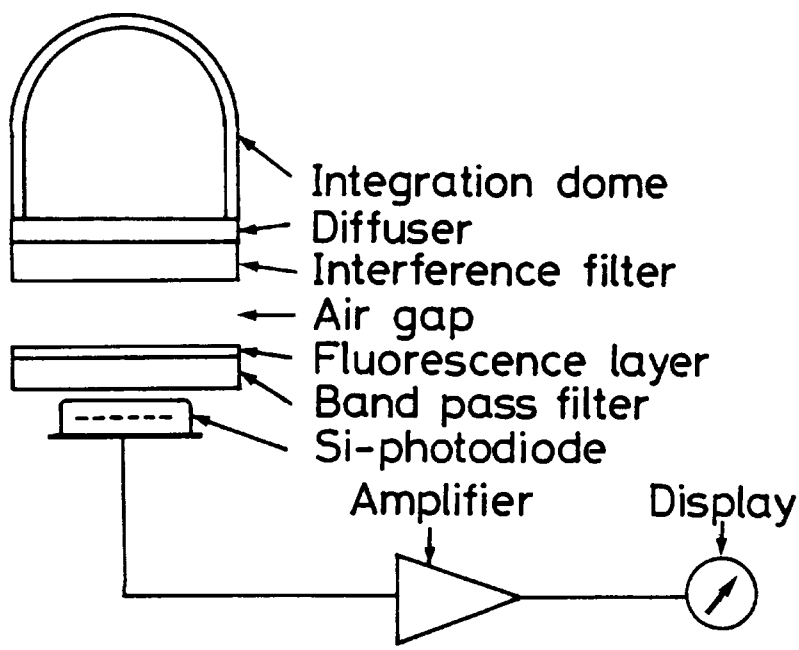

Fig. 1. Diagram of the newly designed physical UV-B dosimeter.

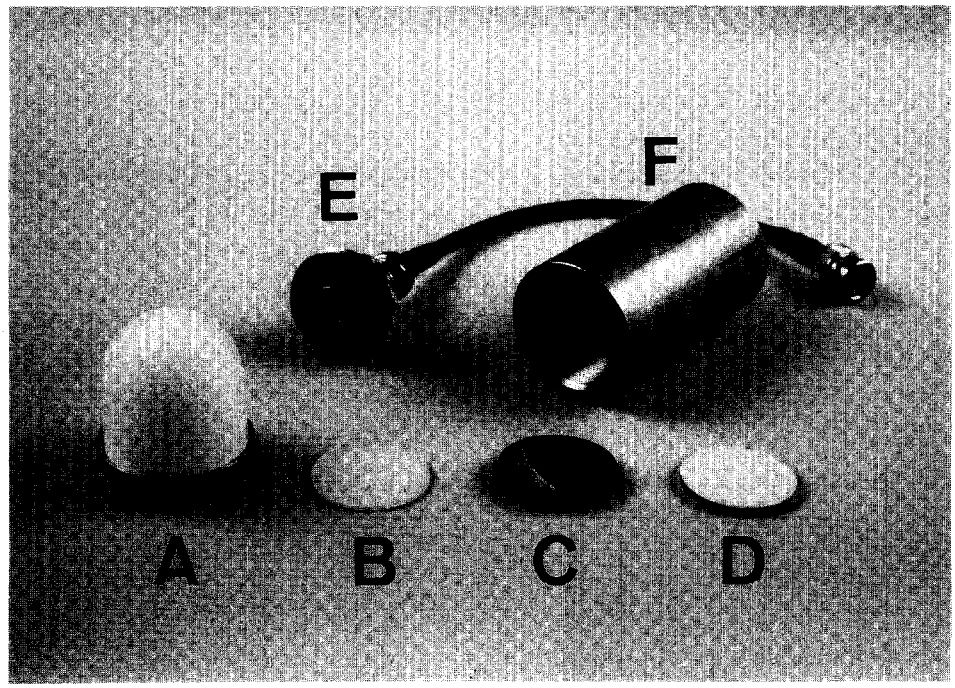

Fig. 2. Components of the photo-detecting probe of the prototype, A: Angular integration dome (Teflon), B: Diffuser (Teflon sheet on a quartz plate), C: Interference filter (KUVB-298), D: Fluorescence layer (SPD-2) coated on a band pass filter composed of a blue-filter (B480) and a sharp cut filter (L-42), E: Silicone-photodiode (S1226-8BK) and F: Body of the detecting probe.

(A) An integration dome made of Teflon to collect solar UV-B covering whole solid angles, (B) a diffuser (Teflon sheet, thickness 0.1 mm) and (C) an interference filter (KUVB-298, Kōshin Kougaku Co., Hadano, Japan) with an air-gap which enables adjustment of the overall spectral response, (D) a fluorescence layer (SPD-2, Toshiba) to convert UV-B to visible light which is coated on the surface of a band pass filter composed of a blue filter (B480, Hoya) and a sharp cut filter (L-42, Hoya) to block contaminating light, and (E) a photo-electric transducer (photodiode, S1226-8BK, Hamamatsu Photonics). The components of the dosimeter described above were assembled in a compact body (F in Figure 2). The size of detecting probe of a prototype was 3 cm in diameter, 7 cm in length and 250 g in weight.

The sunlight collected by the angular integration dome is scattered by the diffuser. Angular distribution of the scattered light passing through the interference filter then collected by the fluorescence layer can be controlled by adjusting the distance (air-gap) between the diffuser and the fluorescence layer. The UV-B light which has passed through the interference filter excites the fluorescence layer and the latter emits visible fluorescence having an emission peak at 475 nm with a high quantum yield. The emitted visible light which passes through the band pass filter and the sharp cut filter is detected by a silicone-photodiode.

Adjustable spectral sensitivity

The property[16] of thin layer interference filter is that the peak transmitting wavelength shifts to shorter wavelengths with increasing incident angle: thus, transmittance at wavelengths shorter than the normal transmitting wavelength increases with decreasing incident angles. The ratio of light flux coming at low incident angles ($<90°$) to that of normal incident angle ($=90°$) will increase when a diffuser is interposed above the interference filter, so that the scattered light passes through the interference filter with incident angles covering geometrically available solid angles, and then arriving at the fluorescence layer. Moreover, the ratio of the light passing through the interference filter can be controlled by changing the air-gap between the diffuser and the fluorescence layer. The range of the incident angle of the light which passed through the interference filter then arrived at the fluorescence layer decreased with increasing distance of air-gap.

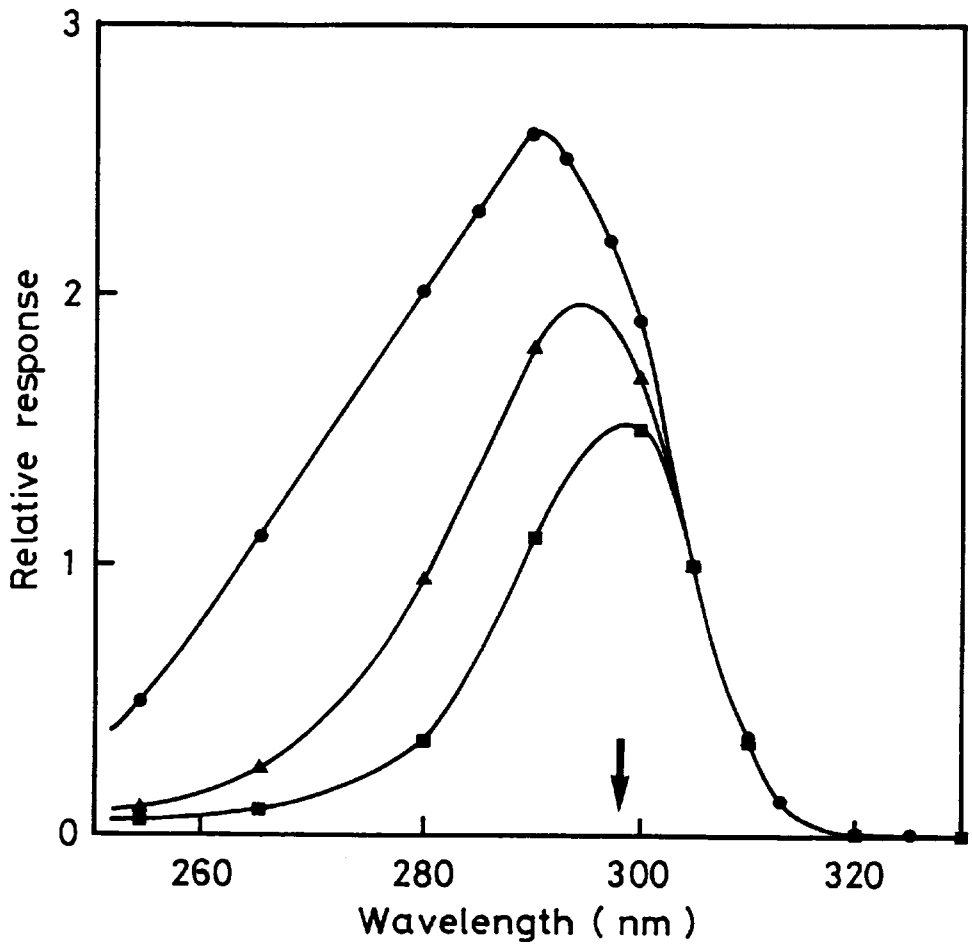

Fig. 3. Change of overall spectral response of the meter by alternation of air-gap. The spectral response was normalized to the value at 305 nm, and the distance between the diffuser and the fluorescence layer is (●) 5 mm, (▲) 18 mm and (■) 34 mm. The arrow indicates the main transmitting wavelength of the interference filter KUVB-298.

Therefore the air-gap can control the shape of the overall transmittance spectrum of the system. When an interference filter KUVB-298 was inserted into the dosimeter, the air-gap could be altered from 2 mm to 35 mm. The change in overall spectral response of the UV-B dosimeter by alternating the distance of the air-gap is shown in Figure 3. The relative spectral responses of the dosimeter in the wavelength range longer than 305 nm is not affected by changing the air-gap, whereas the response is increased greatly by decreasing the air-gap especially in the wavelength range shorter than the main transmitting wavelength of the interference filter (298 nm).

Moreover, the diffuser keeps the angular distribution of light to the interference filter constant even if the incident angle of light coming to the detecting probe head is changed. Thus the overall response of the system is not affected by the change of geometrical condition between light source and diffuser.

Angular response

For monitoring components of sunlight which are harmful to biological materials, it is necessary to measure the light flux covering both direct solar-radiation and diffused sky-radiation, because, at wavelengths around 300 nm, the major part of incident light[17] is composed of sky-radiation. Most types of commercially available radiometers have flat detector surfaces, so that they have cosine type angular responses, and such dosimeters may not fully detect the diffused sky-radiation which comes from lower altitudes in the sky. Installation of an angular integrator should improve this defect, because it collects UV radiation equally from the whole solid angles in the sky. A fish-eye lens made of quartz is desirable for this purpose, but it is very expensive. Thus we used a Teflon hollow hemispheric dome with a straight neck (Figure 1, integration dome), which completely diffuses the light and transfers it into the dome. Angular response of the dosimeter is controlled by neck length of the dome. When neck length was adjusted at 6 mm, error of the angular response (*i.e.* response without cosine function) was within 15% from the ideal response for incident angle between 0° to 90°.

RESULTS AND DISCUSSION

Inactivation action spectrum of bacteriophage T1

The action spectrum of phage T1 was measured in CRM-FM and OLS. A repair deficient strain of *E. coli* Bs-1 was used as an indicator. Survival curves obtained on a semi-logalithmic plot were linear with a small shoulder at every wavelength. In all experimental curves, the extrapolation number was two in accordance with the hit theory. Mean lethal doses D_0 (the dose required to reduce survival to 1/e based on the exponential slope) and inactivation rate constants ($1/D_0$) obtained in several experiments at each wavelengths are listed in Table 1, and the results within the UV-B region are illustrated in Figure 4-a (closed circle). A spectral biological effectiveness for exposure limits reported by WHO[8] (solid line), an erythemal action spectrum informed by CIE[7] (dotted line) and spectral solar irradiance[18] which is affected by the ozone thickness (solid line with shadow) are also shown in the same figure. It can be seen that the action spectrum

Table 1. Mean lethal doses and inactivation rate constants of bacteriophage T1. Phage samples were exposed to monochromatic ultraviolet light wavelength range from 225 nm to 400 nm obtained from a Spectro-irradiator CRM-FM and the Okazaki Large Spectrograph (OLS), *E. coli* Bs-1 was used as host cells. Extrapolation numbers according to the hit theory were 2.0 for each experiment.

Wave-length (nm)	Mean lethal dose D_0 (J/m^2)		Inactivation rate constant $1/D_0$ (m^2/J)	
	CRM-FM	OLS	Experiment*	with UV30**
225	6.80×10^{0}		1.5×10^{-1}	
235	7.72×10^{0}		1.3×10^{-1}	
245	3.33×10^{0}		2.5×10^{-1}	
254	2.53×10^{0}	2.68×10^{0}	4.5×10^{-1}	
265	1.72×10^{0}		5.8×10^{-1}	
275	2.17×10^{0}		5.2×10^{-1}	
280		2.32×10^{0}	3.6×10^{-1}	
285	5.14×10^{0}		2.1×10^{-1}	
290		1.11×10^{1}	8.5×10^{-2}	3.2×10^{-3}
295	3.14×10^{1}		2.9×10^{-2}	4.5×10^{-3}
300	1.52×10^{2}	2.46×10^{2}	7.0×10^{-3}	2.7×10^{-3}
305			1.4×10^{-3}	8.3×10^{-4}
310		3.40×10^{3}	3.0×10^{-4}	2.2×10^{-4}
315		1.22×10^{4}	8.4×10^{-5}	6.7×10^{-5}
320		2.37×10^{4}	3.5×10^{-5}	2.9×10^{-5}
325		5.83×10^{4}	1.7×10^{-5}	1.5×10^{-5}
330		1.35×10^{5}	1.0×1.0^{-5}	8.8×10^{-6}
335		1.40×10^{5}	6.2×10^{-6}	5.8×10^{-6}
340		2.61×10^{5}	4.0×10^{-6}	3.6×10^{-6}
345			2.8×10^{-6}	2.5×10^{-6}
355			1.5×10^{-6}	1.3×10^{-6}
365		1.27×10^{6}	7.9×10^{-7}	7.1×10^{-7}
375			4.0×10^{-7}	3.6×10^{-7}
385			2.2×10^{-7}	2.0×10^{-7}
395			1.1×10^{-7}	1.0×10^{-7}
400		1.24×10^{7}	8.1×10^{-8}	7.3×10^{-8}

* Interpolated value by smoothing on a semi-logalithmic chart.

** Estimated value when phages were covered with UV-30 (t = 1.4 mm) filter.

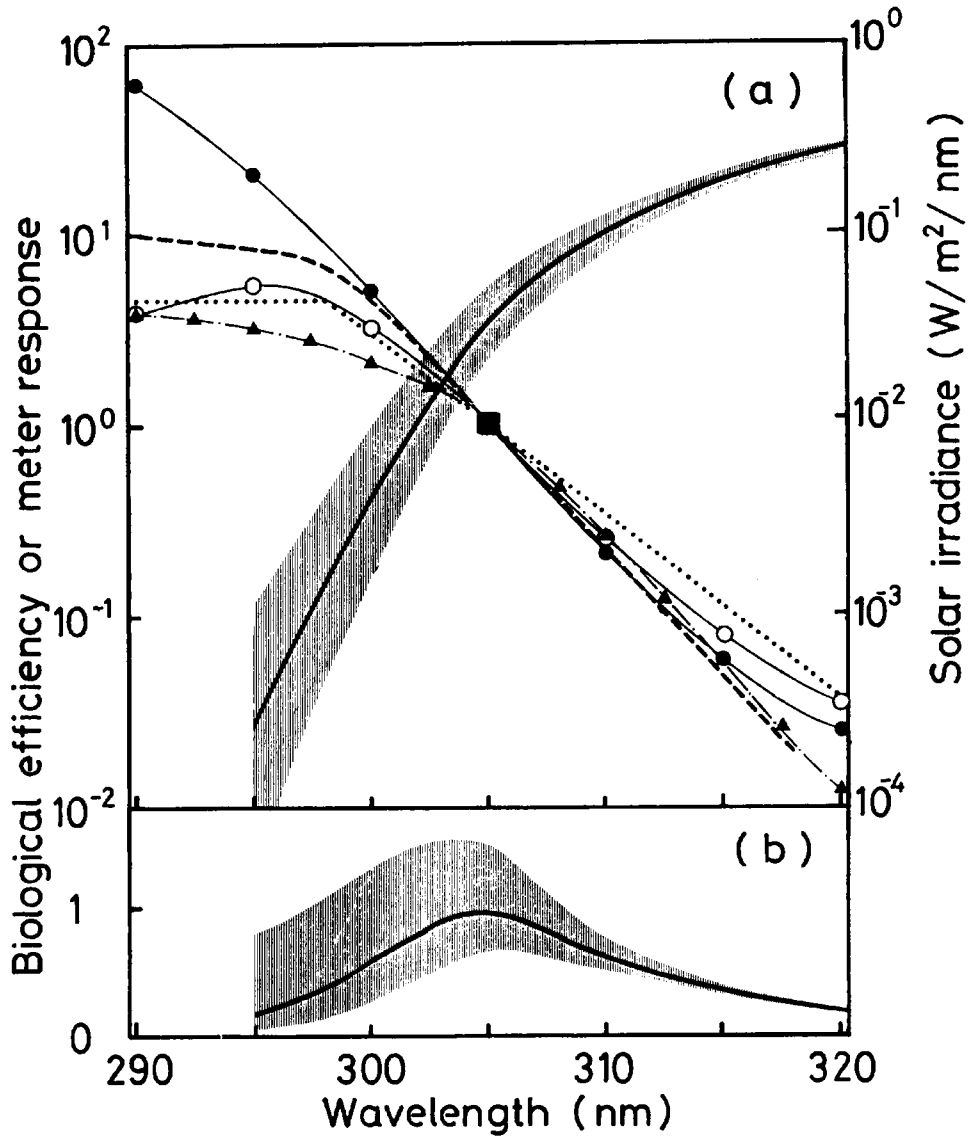

Fig. 4. (a); Biological action spectra, spectral responses of the newly developed UV-B dosimeter and spectral solar irradiances. Inactivation action spectrum of phage T1 (●), inactivation action spectrum of phage T1 covered with UV-30 (t = 1.4 mm) filter (○) and spectral response of the UV-B meter fitted to the inactivation of T1 (▲). Biological effectiveness for exposure limits reported by WHO[8] (– – – –) and an action spectrum of erythema recommended by CIE[7] (·····). Spectral irradiance of UV on the ground[18] (———) at solar altitude Z = 60° at normal value (320 Dobson) of total ozone. Upper and lower envelope of the shadow indicates variation of the irradiance when total ozone is 240 and 400 Dobson, respectively. (b); Relative killing efficiency of sunlight on bacteriophage T1. The efficiency is affected (shadow) by ozone thickness (the symbols are the same as solar irradiance). The values were calculated as products of spectral solar UV irradiance and inactivating action spectrum of phage T1.

of phage T1 is similar to that of biological effectiveness and/or erythema. Also, phage action spectrum is very close to biological action spectra such as dimer formation in DNA[19], lethality and mutagenesis of *E. coli*[19], inactivation of various cells[20] and DNA absorption[21].

Net potential effect of solar UV on biological material is given by the product of intensity of solar UV at each wavelength and the efficiency of the monochromatic light to cause any biological effect of interest. Figure 4-b show the relative spectral effectiveness of sunlight obtained in such a way, in which the action spectrum of biological material was taken from the data of phage T1. It seems that the efficiency of sunlight upon phage T1 has a peak at 305 nm at normal ozone thickness (solid line, 320 Dobson unit), and that the efficiency below 310 nm is greatly altered (shadow) by change in the thickness (240–400 Dobson) of the ozone. Similar results were reported by Setlow[22]. Thus, in order to evaluate accurately the net biological effect of sunlight which is affected by the ozone layer, it is a prerequisite that the response of UV dosimeter should follow the spectrum described above at least in this wavelengths region. The action spectrum of phage T1 at wavelengths below 300 nm are varied from that of erythema[7,23] or biological effectiveness of WHO[8], however the action spectrum of phage T1 could fit the action spectra of some biological materials. The estimated values of the apparent action spectrum of phage T1 when the irradiation cell was covered with an UV-cut filter (UV-30, 1.4 mm^t, Hoya) are shown in Table 1 and Figure 4-a (open circle) as an example. This result shows that the action spectrum of phage T1 fits the erythemal action spectrum in the entire wavelength range of UV-B, and it also corresponds to the biological effectiveness reported by WHO. This indicates that phage T1 is not only useful as an erythemal dosimeter but may also be used as a dosimeter for measuring other biological effects if fitted with an appropriate UV filter.

Seasonal change of killing efficiency of sunlight on phage T1

Outdoor experiments were carried out throughout one year at around noon (approximately from 11 a.m. to 1 p.m.) in Isehara (139.5°E, 35.5°N), Kanagawa, about 50 km south-west of Tokyo. In every experiment, survival versus exposure time gave a linear survival curve on semi-logarithmic scale plot with an extrapolation number m = 2.0, as in the case of exposure to monochromatic UV light. Table 2 show the cumulative survival data of 50 series of such experiments on comparatively fine days. Killing efficiencies of solar UV light were determined as reciprocals of D_0 which is expressed in exposure time and/or sunburn units. The killing efficiencies from April to October (summer) were significantly higher than those from December to February (winter) for expressions either in exposure time or sunburn units. Mean values and standard deviations of these values were 3.71 ± 1.55 hr^{-1} and 1.94 ± 0.47 SU^{-1} in summer and 0.63 ± 0.28 hr^{-1} and 0.90 ± 0.15 SU^{-1} in winter, respectively. The ratios of killing efficiency of sunlight in summer to those in winter are 5.94 (=3.71/0.63) and 2.16 (=1.94/0.90) calculated on the basis of exposure time and sunburn unit, respectively. Thus, the exposure of sunlight per unit time is about 6 times more effective in summer than in winter. This ratio of killing efficiency is in a good agreement with that of genotoxicity of *Bacillus subtilis* spores[9] at Tokyo.

Seasonal change of killing efficiency of sunlight as expressed by exposure time (hr^{-1}) and by sunburn unit (SU^{-1}) are shown in Figure 5-a and -b, respectively. Also, seasonal change of

Table 2. Seasonal change of phage survival exposed to natural sunlight during one year (1983-84). The m numbers and mean lethal doses (D_0) calculated from the reading of the R-B meter in sunburn unit (SU) and exposure time in hour unit (hr) based on the hit theory, and killing efficiencies of sunlight ($1/D_0$).

No.	Date		m**	D_0**		Killing Efficiency	
	M	D		(SU)	(hr)	(SU^{-1})	(hr^{-1})
1	4	13	1.728	0.547	0.291	1.827	3.434
2	4	13*	2.057	0.467	0.707	2.142	1.413
3	4	14	1.876	0.564	0.303	1.772	3.295
4	4	18	2.443	0.441	0.239	2.266	4.193
5	4	18*	1.880	0.414		2.415	
6	4	20	2.094	0.644	0.247	1.554	4.055
7	4	26	2.109	0.860	0.312	1.163	3.210
8	5	9	2.032	0.626	0.295	1.598	3.388
9	5	10	1.888	0.545	0.337	1.834	2.971
10	5	11	1.958	0.750	0.333	1.334	3.001
11	5	12	2.015	0.628	0.654	1.593	1.529
12	5	25	2.184	0.360	0.581	2.778	1.723
13	6	2	2.058	0.490	0.219	2.039	4.567
14	6	9	2.031	0.557	0.232	1.795	4.309
15	6	10	1.963	0.812	0.738	1.232	1.355
16	6	14	2.440	0.376	0.144	2.662	6.949
17	6	22	1.988	0.533	0.227	1.878	4.412
18	6	29	2.004	0.560	0.271	1.785	3.694
19	7	1	2.030	0.582	0.298	1.719	3.353
20	7	13	1.915	0.549	0.260	1.821	3.843
21	7	14	2.013	0.387	0.161	2.584	6.201
22	7	19	2.108	0.668	0.355	1.498	2.816
23	8	4	1.722	0.576	0.320	1.735	3.123
24	8	9	2.103	0.680	0.224	1.471	4.458
25	9	1	2.084	0.358	0.159	2.794	6.285
26	9	6	1.919	0.513	0.135	1.948	7.404
27	10	3	2.059	0.350	0.343	2.854	2.911
28	10	4	2.092	0.479	0.431	2.089	2.318
29	11	2	2.205	0.590	0.663	1.694	1.508
30	11	7	2.036	0.574	0.592	1.743	1.691
31	11	8	2.040	0.772	0.764	1.296	1.309
32	11	21	1.994	0.504	0.710	1.984	1.409
33	11	22	2.071	0.676	1.024	1.480	0.977
34	12	10	2.122	0.877	1.595	1.140	0.627
35	12	13	2.049	1.249	2.906	0.800	0.344
36	12	16	2.054	1.485	3.299	0.674	0.303
37	1	13	2.072	0.994	1.875	1.006	0.533

38	1	17	2.003	1.123	1.291	0.891	0.775
39	2	2	2.011	1.232	1.580	0.812	0.633
40	2	3	2.048	0.935	2.597	1.070	0.385
41	2	7	2.078	1.204	1.720	0.831	0.582
42	2	8	1.953	1.533	1.433	0.652	0.698
43	2	21	2.024	1.164	1.141	0.859	0.876
44	2	27	1.960	0.913	0.731	1.095	1.369
45	2	28	1.921	1.093	2.667	0.915	0.375
46	3	1	2.014	0.897	0.925	1.115	1.081
47	3	6	2.000	1.305	1.403	0.767	0.713
48	3	9	2.123	1.056	1.509	0.947	0.663
49	3	17	2.104	0.769	0.611	1.300	1.638
50	3	23	2.147	0.730	0.541	1.370	1.850
All		MEAN	2.036	0.740	0.824	1.572	2.460
		SD	0.125	0.303	0.772	0.587	1.187
Apr. to Oct.		MEAN	2.028	0.547	0.327	1.935	3.712
		SD	0.156	0.130	0.160	0.466	1.546
Dec. to Feb.		MEAN	2.025	1.150	1.903	0.895	0.625
		SD	0.056	0.201	0.753	0.151	0.282

* data obtained after 1 p.m.

** $SF = m \cdot \exp(-D/D_0)$, at linear portion of each survival curve, where SF is survival fraction, D is exposure in hour or sunburn unit, and m is the extrapolation number according to the hit theory.

effective ozone thickness is shown in Figure 5-c, where the effective ozone thickness was calculated as products of the averaged data of total ozone (column density of O_3)[24] at geographic latitude 35°N and the air mass which is given by the solar altitude at noon. Seasonal change of the effective ozone thickness (Figure 5-c) and that of the killing efficiency of sunlight (Figure 5-a and -b) show a good inverse correlation: the killing efficiencies were high in summer (Apr. to Oct.) when the effective ozone layer was thin, and the efficiencies were low when the effective ozone layer was thick in winter (Dec. to Feb. of the next year). Therefore, it is clear that the ozone layer must protect phages from killing by sunlight. The variation of the killing efficiencies in short term may be caused by daily variation of total ozone and other atmospheric conditions such as clouds or aerosols which absorb and/or scatter the UV-B light.

Evaluation of the UV-B dosimeter

The spectral response of the dosimeter which fits to the inactivation action spectrum of phage T1 is shown in Figure 4-a (triangles). The spectral response of the dosimeter at wavelengths range below 300 nm are insufficient for accurate measurement of efficiency of sunlight on phage T1. Still, sunlight in this wavelength range takes only a small part of the total efficiency upon phage

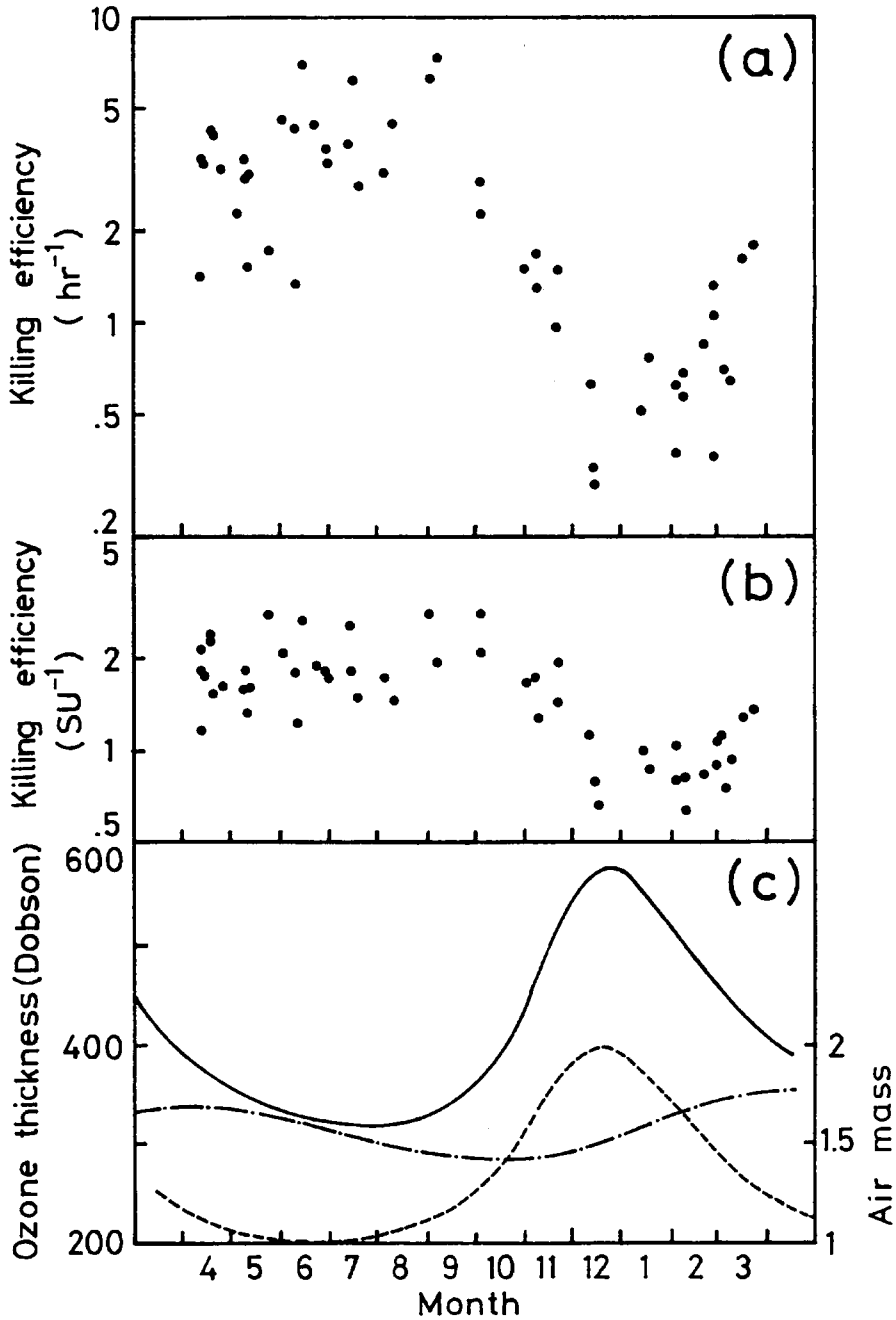

Fig. 5. Seasonal change of killing efficiency of sunlight upon bacteriophage T1. Outdoor experiments were carried out at around noon in Isehara. Japan (139.5°E, 35.5°N). Repair deficient strain *E. coli* Bs-1 was used as host cells. the ordinates in (a) and (b) are expressed in reciprocal values of exposure time and sunburn unit, respectively. (c); Seasonal change of effective ozone thickness (——). The effective ozone thickness is calculated as the product of total ozone[24] (—·—·—) and air mass which indicates the light path through the ozone layer (-------).

T1 when ozone thickness is ordinary. It may be preferable than the dosimeter should be hypersensitive in wavelengths longer than 310 nm, in which the solar irradiance is strong but biological effect is very small. So that small change of UV intensity caused by ozone in shorter wavelengths of light may not be masked by the sensitivity of the longer wavelengths.

The intensity of UV relative to the total irradiance was measured on both a cloudy (Figure 6-a) and a fine day (Figure 6-b) in June using the novel UV-B dosimeter at Isehara. The output of the UV-B dosimeter generated by natural sunlight was about 1.0 V at noon on a fine day. Under the same conditions, solar irradiance (300–3000 nm) and solar UV-irradiance (300–400 nm) were about 900 W/m^2 and 40 W/m^2, respectively. The results show that the UV-B dosimeter follows the change of the effective ozone thickness depending on the solar zenith as a reciprocal value of air mass (solid line without symbol), but MS-140 UV-radiometer does not. And it was also found that the readings were sensitively influenced by temporal shielding with cloud; again a fact which was not observed by MS-140 UV-radiometer. This UV-B dosimeter followed atmospheric conditions very faithfully, because it was designed to detect the shortest wavelength edge of sunlight on the ground which is greatly affected by the ozone layer, aerosols, clouds

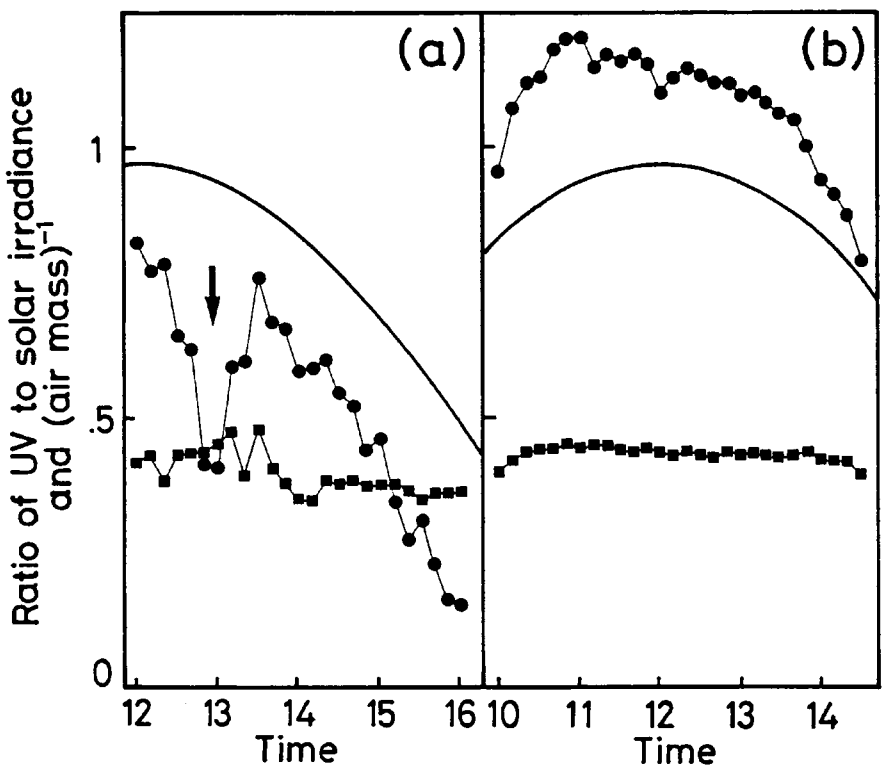

Fig. 6. Change of the ratios of UV-irradiance to solar irradiance. The ratios were measured with the new UV-B dosimeter (1 × [mV]/[W/m^2], —●—) and MS-140 UV-radiometer (10 × [W/m^2]/[W/m^2], —■—), where solar irradiances were measured by MS-140 and MS-801 actinometer. Change of reciprocal value of air mass (——) caused by the solar altitude. (a); On a cloud day, (↓): An unexpected increase of cloud occurred here. (b); On a fine day.

and so on. On the other hand, UV-irradiance measured by MS-140 may reflect only a part of the solar UV-irradiance which is a spectrally unchanged proportion of the solar irradiance.

Output of this UV-B dosimeter and the killing efficiency of natural sunlight on phage T1

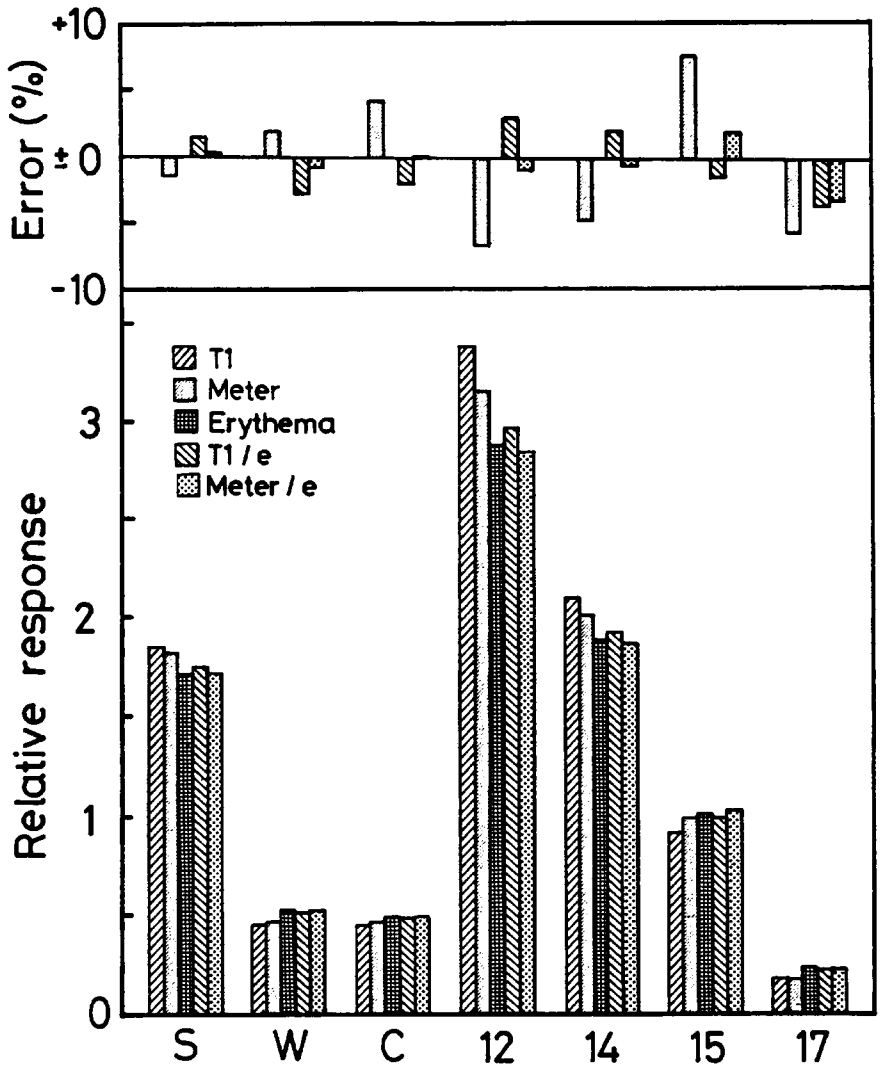

Fig. 7. Simulated responses of dosimeters by solar UV in summer (S), in winter (W), on a cloud day (C) and variation by time on a fine day (12–17). Relative solar efficiencies on materials (bottom) are calculated with the data of spectral irradiance[25] and spectral responses of phage T1 (T1), UV-B dosimeter (Meter), erythema[7] (Erythema), bacteriophage T1 covered with UV-30 filter to fit the erythemal action spectrum (T1/e) and UV-B dosimeter modified to be as an erythemal dosimeter (Meter/e). Responses for each dosimeters and biological materials are normalized to the response for averaged spectral irradiance at noon throughout one year. The discrepancy between ideal responses and dosimeter responses at each condition (top) are indicated as error of "Meter" to "T1" and "T1/e" or "Meter/e" to "Erythema".

was measured several times in summer in the same way described previously. In this experiment, the mean lethal dose (D_0) was calculated from the output of the dosimeter, and it was 0.24 V·hr. Where V·hr is an integrated value of the output and the time. Under the same conditions, the mean lethal dose was 0.26 hr or 0.45 SU when it was expressed in exposure time or in sunburn units, respectively. According to the results, exposure of 1 hour at an intensity of 1.0 V by the UV-B dosimeter, 4 lethal events were induced in phage, giving 8 lethal damages since the extrapolation number was found to be 2.0.

Simulation of responses to sunlight

Responses of dosimeters and biological efficiencies of sunlight were simulated with the data of spectral irradiance and action spectrum or spectral responses, and the results are shown in Figure 7. In this simulation, the index of overall response I was calculated from the following formula,

$$I = \Sigma I_\lambda \cdot E_\lambda$$

where, I_λ is the spectral irradiance and E_λ is the spectral response of each instrument or biological system. The wavelength ranges λ were integrated from 290 nm to 400 nm. The spectral responses of phage T1, erythema[7] and new UV-B dosimeter were used and calculated with the data of the spectral irradiance. The data of spectral irradiance on a horizontal plane was measured by Habu *et al.*[25] at Tanashi, Tokyo. From their results some data were selected and used in the calculation as follows. The spectral irradiance measured on fine days (cloud cover was less than 3) at around noon (from 11:00 a.m. to 12:30 p.m.) was selected from the data, then divided into three groups and averaged. One group included measurements made within one year (annual), the second group, the summer (S) group included 12 measurements made from April to October, and the winter (W) group was made up of 19 measurements done from December to the following February. The data measured at 11:49 in March 6, 1979 were used as data for cloudy ((C); cloud cover was 10). Data measured at 11:44, 14:02, 15:11 and 17:00 in June 22, 1979 (12, 14, 15 and 17 in Figure 7, respectively) were also used. Results of the calculations for each instrument in absolute values were normalized to 1 with the values obtained from the data of average spectral irradiance throughout the year (annual). In other words, all instruments were calibrated against each other on an average fine day at noon. The results show that the output of the new UV-B dosimeter gives a good index of the killing efficiency of sunlight on phage T1 within an 8% error at every simulated condition.

On the other hand, when phage T1 covered with UV-30 filter and/or new UV-B dosimeter tuned for erythemal dosimeter, the error of the index value from the ideal response of erythema (erythemal action spectrum of CIE is thought to give the ideal erythemal index) is less than 4% for both dosimetry systems at simulated conditions. This indicates that both dosimetry systems are very good indices of erythema by sunlight, and also, that the physical dosimeter can be calibrated by the phage-filter system without any absolute spectral measurement of sunlight and dosimeter.

ACKNOWLEDGMENTS

We are grateful to Dr. N. Ishii of the Department of Molecular Biology, Dr. H. Maezawa of the Department of Radiation Oncology, Tokai University School of Medicine, Dr. M. Watanabe of the National Institute of Basic Biology and Mr. Y. Miyake of EKO Instruments Trading Co., Ltd. for their advices. The authors also acknowledge Mr. F. Meguro, Mr. K. Nakajima, Mr. S. Takeshita and Mr. M. Kubota for their kind co-operation, and Mr. T. Sugimoto of Toshiba Co. for gift of fluorescence powder SPD-2. We wish to thank Mrs. Nadia El Borai (M.Sc.) for correcting the English text. This study was supported in part by the National Institute of Basic Biology Cooperative Research Program of the Okazaki Large Spectrograph Laboratory (86-532, 87-526, 88-518), and also was supported in part by the Science Research Promotion Fund by the Japan Private School Promotion Foundation.

REFERENCES

1. Chubachi, S. (1984) Preliminary result of ozone observations at Showa station from February 1982 to January 1983. In "Proceedings of the Sixth Symposium on Polar Meteorology and Glaciology", Ed. K. Kusunoki, pp. 13-19, National Institute of Polar Research, Tokyo.
2. Farman, C.J., Gardinar, B.G. and Shanklin, J.D. (1985) Large losses of total ozone in Antarctica reveal seasonal ClO_x/NO_x interaction. Nature **315:** 207-210.
3. Solomon, S., Garcia, R.R., Rowland, F.S. and Waebbles, D.J. (1986) On the depletion of Antarctic ozone. Nature **321:** 755-758.
4. UNEP (1987) Montreal Protocol on Substances That Deplete the Ozone Layer, Final Act, United Nations Environment Program.
5. WMO Global Ozone Research and Monitoring Project (1986) Atmospheric Ozone 1985, Vol. I, II, III, Report No. 16, World Meteorological Organization, Geneva.
6. WHO (1979) Environmental health criteria 14: Ultraviolet radiation. pp. 110, World Health Organization, Geneva.
7. CIE (1987) A reference action spectrum for ultraviolet induced erythema in human skin. CIE Journal **6:** 17-22.
8. WHO (1982) Environmental health criteria 23: Lasers and optical radiation. pp. 90-113, World Health Organization, Geneva.
9. Munakata, N. (1989) Genotoxic action of sunlight upon *Bacillus subtilis* spore: Monitoring studies at Tokyo, Japan. J. Radiat. Res. **30:** 338-351.
10. Tyrrell, R.M. (1978) Solar dosimetry with repair deficient bacterial spores: Action spectra, photoproduct measurements and a comparison with other biological systems. Photochem. Photobiol. **27:** 571-579.
11. Sato, K., Sano, S., Ikenaga, M. and Aoki, T. (1984) Estimation of minimum erythema time of patients with xeroderma pigmentosum based on measurement of solar radiation. Skin Res. **26:** 501-509. (in Japanese).
12. Watanabe, M., Furuya, M., Miyoshi, Y., Inoue, Y., Iwahashi, I. and Matsumoto, K. (1982) Design and performance of The Okazaki Large Spectrograph for photobiological research. Photochem. Photobiol. **36:** 491-498.
13. Watanabe, M. (1985) The Okazaki Large Spectrograph and its application to action spectroscopy. In "Photobiology 1984", Eds. J.W. Longworth, J. Jagger and W. Shropshin Jr., pp. 37-44, Praeger, New York.
14. Nakayama, Y., Morikawa, F., Fukuda, M., Hamano, M., Toda, K. and Pathak, M.A. (1972) Monochromatic radiation and its application – Laboratory studies in the mechanism of erythema and pigmentation induced by psoralen. In "Sunlight and Man" Ed. Fitzpatrick, T.B., pp. 591-611, University of Tokyo Press, Tokyo.

15. Berger, D.S. (1976) The sunburning ultraviolet meter: Design and performance. Photochem. Photobiol. **24:** 587-593.
16. Hadley, L.N. and Dennison, D.M. (1947 and 1948) Reflection and transmission interference filters. Part I. Theory., Part II. Experimental, comparison with theory, results. J. Opt. Soc. Amer. **37:** 451-465 and **38:** 483-496.
17. CIE (1972) Recommendations for the integrated irradiance and the spectral distribution of simulated solar radiation for testing purposes, Publication CIE No. 20 (TC-2.2), pp. 1-54, International Commission on Illumination, Paris.
18. WMO Global Ozone Research and Monitoring Project (1977) Report of the meeting of experts on UV-B monitoring and research. pp. 1-9, World Meteorological Organization, Geneva.
19. Peak, M.J., Peak, J.G., Moehring, M.P. and Webb, R.B. (1984) Ultraviolet action spectra for DNA dimer induction, lethality, and mutagenesis in *Escherichia coli* with emphasis on the UVB region. Photochem. Photobiol. **40:** 613-620.
20. Jagger, J.A. (1985) Mid-UV actions. In "Solar-UV Actions on Living Cells", pp. 103-112, Praeger, New York.
21. Sutherland, J.C. and Griffin, K.P. (1981) Absorption spectrum of DNA for wavelengths greater than 300 nm. Radiat. Res. **86:** 399-410.
22. Setlow, R.B. (1974) The wavelengths in sunlight effective in producing skin cancer: A theoretical analysis. Proc. Natl. Acad. Sci. USA **71:** 3363-3366.
23. Parrish, J.A., Jaenicke, K.F. and Anderson, R.R. (1982) Erythema and melanogenesis action spectra of normal human skin. Photochem. Photobiol. **36:** 187-191.
24. Dütsch, H.U. (1980) Ozone in the atmosphere. Does stratosphere pollution endanger the ozone layer? Neujahrsblatt Naturforschende Gesellsch. Zürich **182:** 1-48.
25. Habu, M., Suzuki, M. and Nagasaki, T. (1981) Measurement of the solar spectral irradiance at Tanashi, Tokyo (I, II and III). Researches of the Electrotechnical Laboratory No. 812, 813 and 830, Electrotechnical Laboratory, Ibaraki, Japan. (in Japanese).